Efficient Visible Light Degradation of Rhodamine B by a Photo-Electrochemical Process Based on a Bi_2WO_6 Nanoplate Film Electrode

Jinpo Li,[†] Xi Zhang,[†] Zhihui Ai,[†] Falong Jia,[†] Lizhi Zhang,*[,†] and Jun Lin*[,‡]

Key Laboratory of Pesticide and Chemical Biology of Ministry of Education, College of Chemistry, Central China Normal University, Wuhan 430079, People's Republic of China, and Department of Chemistry, Renmin University of China, Beijing 100872, People's Republic of China

Received: January 26, 2007; In Final Form: March 5, 2007

In this paper, a Bi_2WO_6 nanoplate film electrode was prepared by a hydrothermal method, combined with a spin coating technique. A photoelectrochemical (PEC) oxidation system based on this electrode was then constructed to degrade rhodamine B (RhB) in aqueous solution under visible light ($\lambda > 420$ nm). The PEC system based on Bi_2WO_6 nanoplate film electrode could degrade 87.2% of RhB with concentration of 5 mg/L in 120 min, operated at low voltage and under visible light irradiation, whereas only 36.8% and 39.5% degradation of RhB were observed for electro-oxidation process (EC) and photocatalytic oxidation process (PC), respectively, operated under the same condition. These results revealed a significant synergetic effect on degrading RhB via electro-oxidation and photocatalysis under visible light irradiation. A possible mechanism for this synergetic degradation of RhB was proposed on the basis of characterization results. Meanwhile, the degradation pathway of RhB during PEC under visible light irradiation was also discussed. This study provided an effective approach for aqueous organic pollutant removal by utilizing solar light.

Introduction

Over the last few decades, various technologies have been developed for wastewater treatments, including various pollutants degradation strategies and improvement in the degradation efficiency.[1] There has been growing interest in the application of photocatalysis toward the treatment of polluted water.[2−6] In order to avoid the separation of the used catalyst particles in the slurry system, many reports have dealt with the use of supported photocatalysts, especially those immobilized over conducting substrates. It has been proven that the immobilization of photocatalysts on conducting substrates can improve the efficiency of organics degradation through imposing a bias voltage.[7−10]

Heterogeneous semiconductor photocatalytic oxidation is one of the advanced oxidation technologies. It has received increasing attention for over three decades for purifying a great variety of environmental pollutants in water and air.[11−13] In spite of numerous approved patents related to heterogeneous photocatalysis, the development of practical water treatment systems has not yet been successfully achieved because of the rapid recombination of photogenerated electron and hole.[14] Thus, it is of great interest for improving the photocatalytic activity of semiconductors for degradation of organic compounds in water and air. An attractive process popularized in the past few years for degrading organic pollutants is the combination of electrochemical and photochemical technologies, called the photoelectrochemical (PEC) process. PEC takes advantage of the heterogeneous photocatalytic process by applying a biased voltage across a photoelectrode on which the catalyst is supported, which has proven to be an efficient method in degrading organic contaminants in aqueous solutions.[3,15,16] In a PEC system, photoelectrons and photoholes can be well separated under the influence of an applied electric field.[17] In most PEC oxidation systems, a particulate TiO_2 film electrode is usually used as a photoanode by coating TiO_2 nanoparticles on supporting media such as a conducting glass or a metallic material. In these systems based on TiO_2 film electrodes, UV light must be used in order to excite TiO_2.[18] Recently, Zhu and co-workers developed a PEC system based on a porous $ZnWO_4$ film electrode and observed synergetic degradation of RhB between electrochemical oxidation and photocatalysis under UV light.[19] To the best of our knowledge, there have been few reports on the study on PEC degradation of organic pollutants under visible light irradiation.[20] In view of the efficient utilization of visible light, the largest proportion of the solar spectrum and artificial light sources, it is of great importance to develop some PEC systems effectively working under visible light.

More recently, it has also been reported that Bi_2WO_6 semiconductor is an excellent photocatalyst for water splitting and photodegradation of organic compounds under visible light irradiation.[21−25] For example, Zou and his co-workers reported that Bi_2WO_6 could degrade $CHCl_3$ and CH_3CHO under visible light irradiation.[26] In this study, we developed a novel PEC system based on a Bi_2WO_6 nanoplate film electrode. This PEC system could effectively degrade a model refractory organic dye pollutant rhodamine B (RhB) under visible light ($\lambda > 420$ nm). Moreover, we observed a synergetic effect in degrading RhB via electro-oxidation and photocatalysis under visible light. After this manuscript was submitted, we noticed an article in press which reported on photoelectrocatalytic degradation of 4-chlorophenol on Bi_2WO_6 nanoflake film electrode under visible light irradiation by Zhu and co-workers.[27] Obviously, there were many differences between this study and Zhu's. For instance, we used a spin coating method to prepare film electrode.

* Corresponding authors. E-mails: L.Z., zhanglz@mail.ccnu.edu.cn; J.L., jlin@chem.ruc.edu.cn. Tel/Fax: +86-27-6786 7535.
[†] Central China Normal University.
[‡] Renmin University of China.

10.1021/jp070694z CCC: $37.00
Published on Web 04/13/2007

Meanwhile, target pollutant and visible light wavelength in our study were different. More importantly, we explained the synergetic effect between EC, PC, and PEC in more detail and studied the equivalent circuit diagram of the electrochemical impedance spectra. This diagram is very important for design the PEC reactor for wastewater treatment in environmental engineering.

Experimental Section

Reagents. Na_2SO_4, $NH_3{\cdot}H_2O$, H_2O_2, NaOH, $Bi(NO_3)_3{\cdot}5H_2O$, Na_2WO_4, and H_2SO_4 were of analytical grade and used as received without further purification. Indium−tin oxide (ITO) glass (thickness: 1.1 mm; sheet resistance: 5 Ω/cm^2) was purchased from Southern Glass Co. Ltd (China). Deionized water was used throughout the experiments.

Preparation of Bi_2WO_6 Nanoplate Film Electrodes. The ITO glass (2.0 cm × 1.5 cm) was rinsed in an ultrasonic bath with distilled water for 15 min, and then cleaned by immersing in a mixture solution of $NH_3{\cdot}H_2O$ and H_2O_2 for 20 min under 80 °C. The volume ratio of NH_3:H_2O_2:H_2O was 20:40:100. After the rinse procedure was repeated, the ITO glass was finally dried in air.

The Bi_2WO_6 particles were synthesized by a hydrothermal process.[25] $Bi(NO_3)_3{\cdot}5H_2O$ and Na_2WO_4 with an equal stoichiometry were first dissolved in 150 mL of distilled water. After stirring for 15 min, the slurry solution was then transferred into a 100-mL autoclave with a Teflon liner. The autoclave was maintained at 150 °C for 24h and then air-cooled to room temperature. The yellow precipitate was collected and washed with deionized water thoroughly. The as-prepared Bi_2WO_6 sample was dried at 100 °C for 5 h.

The Bi_2WO_6 nanoplate film electrode was prepared by a spin coating method. A 0.1 g of as-prepared Bi_2WO_6 powder and 0.5 mL of water was milled in the glass mortar for 10 min; then 0.5 mL of terpineol was added to the resulting slurry and mixed by milling until Bi_2WO_6 particle was well dispersed. The final suspension was dropped on the surface of the ITO to obtain Bi_2WO_6/ITO electrode through spin coating at 2400 rpm for 1 min (ART MICCRA D-3/PA). The Bi_2WO_6/ITO electrode was dried in air at 50 °C for 2h and then calcined at 450 °C for 2h.

Characterization of Bi_2WO_6 Nanoplate Film Electrodes. The Brunauer−Emmett−Teller (BET) surface area (S_{BET}) of the powder was analyzed by nitrogen adsorption in an AUTOSORB-1 (Quantachrome Instruments) nitrogen adsorption apparatus. The samples were degassed at 180 °C prior to nitrogen adsorption measurements. The BET surface area was determined by multipoint BET method using the adsorption data in the relative pressure (P/P_0) range of 0.05−0.3. The morphology of the Bi_2WO_6/ITO electrode was characterized using scanning electron microscopy (SEM) with an accelerating voltage of 20 KV (JSM-5600LV). The Bi_2WO_6/ITO electrode was characterized by X-ray diffraction (XRD) using a diffract meter with Cu Ka radiation (Shimadzu LabX XRD-6000). UV−vis absorbance spectrum of the electrode was measured by using Hitachi U-3010 UV−vis spectrophotometer.

Degradation of RhB with Different Processes. Degradation of RhB was performed in a reactor with double cells (Scheme 1). A 150 mL anodic cell was placed 15 cm away from a 500W Xe lamp with a 420 nm cutoff filter. The separated cathode cell (150 mL) was parallel to the anodic cell. The initial pH of the dye solution was 5−6. Air was purged into the solutions at a flow rate of 5 $L{\cdot}min^{-1}$ in the anodic and cathodal cells, respectively. Before the beginning of experiments, the system was kept in the dark for 30 min to establish absorption/desorption equilibrium between the solution and electrodes. EC and PCE experiments were performed in the anodic cell, using Bi_2WO_6/ITO electrode with the area of 3 cm^2 in 0.005 $mol{\cdot}L^{-1}$ of Na_2SO_4 electrolyte solution under visible light illumination ($\lambda > 420$ nm). The voltage applied in EC and PEC system was 1.2 V. During the whole experiment, the solutions in the anodic and cathodal cells were magnetically stirred. During photocatalytic oxidation process, Bi_2WO_6/ITO electrode only worked as photocatalyst without applying a biased voltage on it. The concentration of RhB was monitored by colorimetry with a U-3310 UV−vis spectrometer (HITACHI) at 30 min intervals of reaction.

SCHEME 1: Schematic Illustration of PEC System[a]

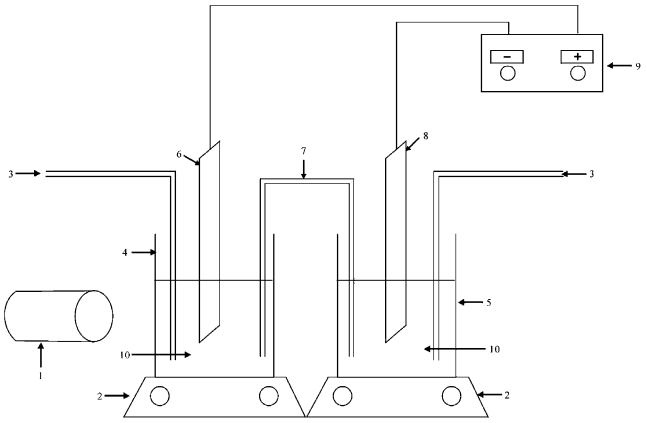

[a] (1) Visible light lamp; (2) magnetic stirrer; (3) air compressor; (4) anodic cell; (5) cathodal cell; (6) Bi_2WO_6/ITO electrode; (7) KCl bridge; (8) Pt cathode; (9) CHI-600A potentiostat; (10) RhB solutions.

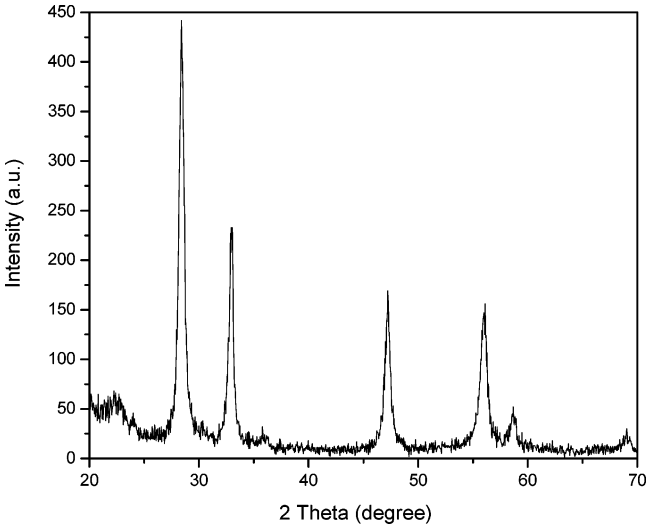

Figure 1. X-ray diffraction pattern of the Bi_2WO_6/ITO electrode.

Results and Discussion

Characterization of Bi_2WO_6 Nanoplate Film Electrodes. The XRD profile of the Bi_2WO_6/ITO electrode was provided in Figure 1. All peaks of the XRD patterns could be indexed according to Bi_2WO_6 (JCPDS file No. 73-1126). The surface morphology of the Bi_2WO_6/ITO electrode was examined by SEM (Figure 2). It was found that the film electrode possessed a uniform, loose, and plate-like structure (Figure 2). The thickness of the plates was in the range of 20−30 nm. These loose structures are believed to favor the absorption of pollutants for the subsequent degradation. The nitrogen adsorption and desorption isotherms (Figure S1, Supporting Information) reveal

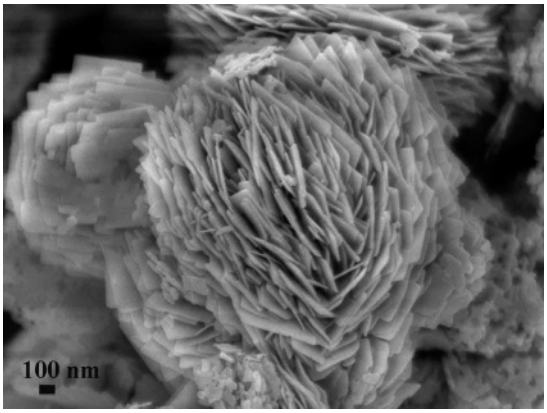

Figure 2. SEM image of the as-prepared Bi_2WO_6/ITO electrode.

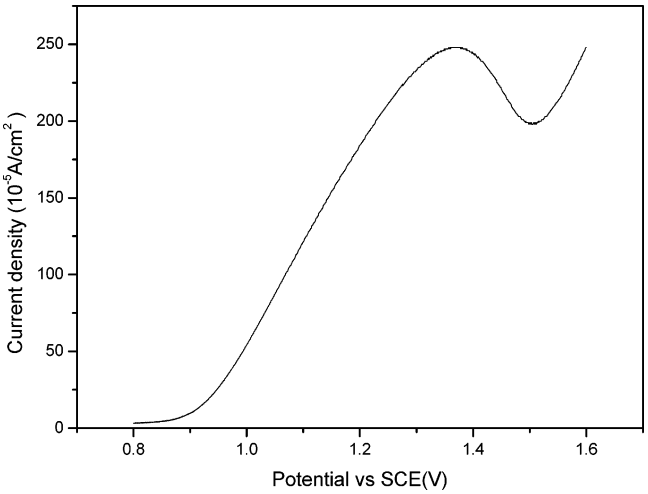

Figure 3. The anodic liner sweep voltammetry of the Bi_2WO_6 nanoplate film electrode in the 0.001 mol·L^{-1} Na_2SO_4 electrolyte solution containing 5 mg·L^{-1} of RhB. pH 7, scan rate 0.1 V/s.

the macroporous structure of the as-prepared Bi_2WO_6 powder. These macropores were produced by the agglomeration of the nanoplates. The BET surface area of the sample was about 6.6 m^2·g^{-1}. UV−vis absorption spectrum of the Bi_2WO_6/ITO electrode is shown in Figure S2 (Supporting Information). Significant increase in the region of absorption wavelengths lower than about 450 nm can be assigned to the intrinsic band gap absorption of Bi_2WO_6. Therefore, Bi_2WO_6 has an intense absorption band with a steep edge in the visible light region. The band gap energy can be estimated from a plot of $(ah\upsilon)^{1/2}$ versus the energy of absorbed light (Figure S3, in Supporting Information). The band gap of the Bi_2WO_6 was then estimated to be 2.62 eV from the onset of the absorption edge, which is close to the value of 2.69 eV reported in literatures.[26] This indicates that Bi_2WO_6 has a suitable band gap as a visible light photocatalyst.

Degradation of RhB with PEC, PC, and EC. The cyclic voltammetry scans of the Bi_2WO_6/ITO electrode in the 0.001 mol·L^{-1} Na_2SO_4 solution containing 5 mg·L^{-1} of RhB were performed at a three electrodes system, with the Bi_2WO_6/ITO as a working electrode, a platinum plate as a counter electrode, and a standard calomel electrode as reference electrode, respectively (Figure 3). It is obvious that the electrochemical degradation of RhB can occur at the voltage more positive than 0.9 V. When the voltage exceeds 0.9 V, the anodic currents increased sharply with the voltage moving positive, which may result from electro-oxidation of RhB accompanied by the evolution of oxygen. Meanwhile, the active species such as

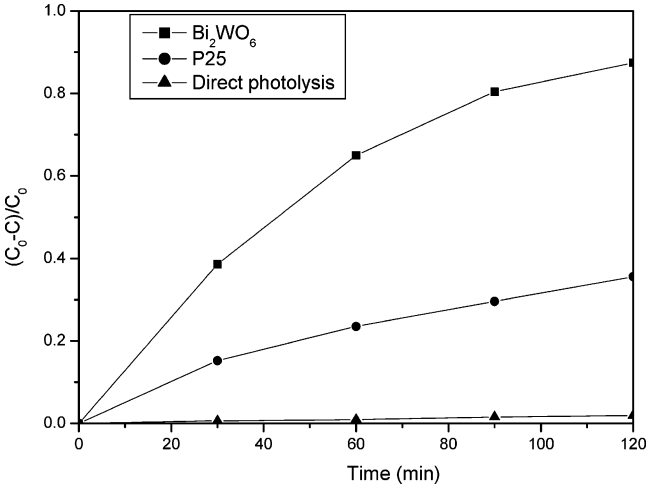

Figure 4. Photoelectrocatalytic degradation of RhB by using different film electrodes (Bi_2WO_6 nanoplate and Degussa TiO_2 P25) and direct photolysis of RhB under visible light irradiation without photocatalysts and a biased voltage.

hydroxyl radicals (·OH) can be formed, which lead to the indirect oxidation of RhB.[28] We found that more hydroxyl radicals in the PEC process were produced than those in other processes (Figure S4, Supporting Information). It was reported that the degradation of RhB by electrochemical oxidation was enhanced by increasing the anodic voltage.[29] Our results also confirmed that the degradation rate of RhB increased with the biased potential increase up to +2.0 V (Figure S5, Supporting Information). This is because the more gradient caused by the positive potential increase could separate holes and electrons better. This separation decreased the combination rate and increased the photocurrent and therefore accelerated the RhB degradation. However, when the voltage was more positive than 1.6 V, decomposition of water would take place, leading to energy waste. Therefore, we applied 1.2 V as the biased voltage during the degradation processes.

Figure 4 shows the temporal concentration changes of RhB in different degradation processes. For comparison, the photoelectrocatalytic degradation of RhB by TiO_2/ITO film electrode was also performed. It was observed that the degradation of RhB over Bi_2WO_6/ITO film electrode was much faster than that in the case of TiO_2/ITO film electrode under the same condition. In contrast, the control experiment without photocatalysts and a biased voltage showed that direct photolysis of RhB under visible light irradiation could be negligible. This confirmed the degradation of RhB over Bi_2WO_6/ITO film electrode was via a photoelectrocatalytic pathway.

Figure 5 shows the degradation of RhB solution by PC, EC, or PEC process in the anodic cell, respectively. During these degradation processes, Bi_2WO_6/ITO acted as the photocatalyst in PC process and the anode in EC or PEC process, respectively. Pt plate was used as the cathode in EC or PEC process. It was found that the removal of RhB reached about 87.2% in PEC system after 120 min of reaction. This value was not only much higher than that in EC system (36.8%) or PC system (39.5%), but also larger than their sum (76.3%). Therefore, there was a significant synergetic effect between electro-oxidation and photocatalytic oxidation of RhB on the Bi_2WO_6 nanoplate film electrode under visible light irradiation. The pseudo-first-order kinetic constants k was calculated and listed in Table 1.

Synergetic Effect in Degrading RhB via Electro-Oxidation and Photocatalysis under Visible Light. In order to investigate the synergetic effect between electro-oxidation and photocata-

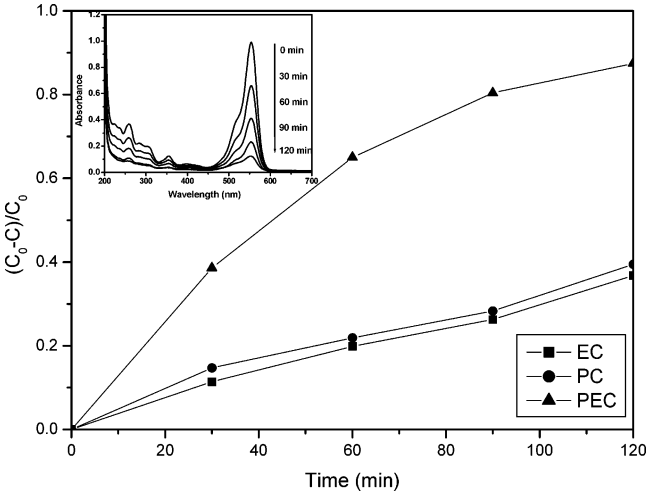

Figure 5. The EC, PC and PEC degradation of RhB in aqueous solution under visible light irradiation and the change of UV−vis absorbance spectra of RhB with irradiation time during PEC process (inset).

TABLE 1: Pseudo-First-Order Kinetic Constants *k* for Degradation of RhB during Different Processes

oxidation system	(min^{-1})	R^2
PEC process	0.0048	0.9941
PC process	0.0026	0.9825
EC process	0.0016	0.9853

lytic oxidation of RhB on the Bi_2WO_6 nanoplate film electrode under visible light irradiation, the electrochemical impedance spectra (EIS) response of the Bi_2WO_6/ITO was performed under EC and PEC conditions (Figure 6). The semicircle-like loop at high frequency was characteristic for the charge-transfer process and the linear part at low frequency resulted from the diffusion-controlled step in the EC reaction (Figure 6a). The diameter of loop at high frequency was largely decreased in PEC process (Figure 6b), compared with that in EC reaction (Figure 6a). Because the diameter of loop at high-frequency reflects the rate of the electrode reaction,[28,29] we concluded that the photoirradiation could increase the electrode reaction in the PEC process, leading to a higher degradation rate of RhB. In addition, only one capacitive loop exists in Figure 6a. This suggests that only the EC reaction take place, whereas two capacitive loops can be observed in the Nynquist plot of PEC process in the Figure 6b, which indicats both PEC and EC reactions happen simultaneously in PEC process under visible light irradiation. The first capacitive response at high- and low-frequency ranges correspond to the reaction of PEC and the process of EC, respectively.

The corresponding equivalent circuit diagram of the EIS in Figure 6 was simulated and presented in Figure 7. In the EC reaction, the charge-transfer resistances R_{ct} of Bi_2WO_6/ITO electrode equaled to the diameter of the semicircle, which was assumed to be about 500 Ω (Figure 7a). However, the R_{ct} (ca. 325 Ω) of the Bi_2WO_6/ITO electrode in the PEC process was much less than that in EC process (Figure 7b). This suggests that it is much easier for the electrode reactions to happen in PEC process under visible light irradiation. The EIS responses of the Bi_2WO_6/ITO under different pH and concentration of RhB solution during PEC process were shown in Figure S6 (Supporting Information). It was found that the size of the arc radius in the EIS Nynquist plot was reduced with increasing either acidity or the concentration of RhB. The size of the arc radius in the EIS Nynquist plot reflects the rate of the electrode

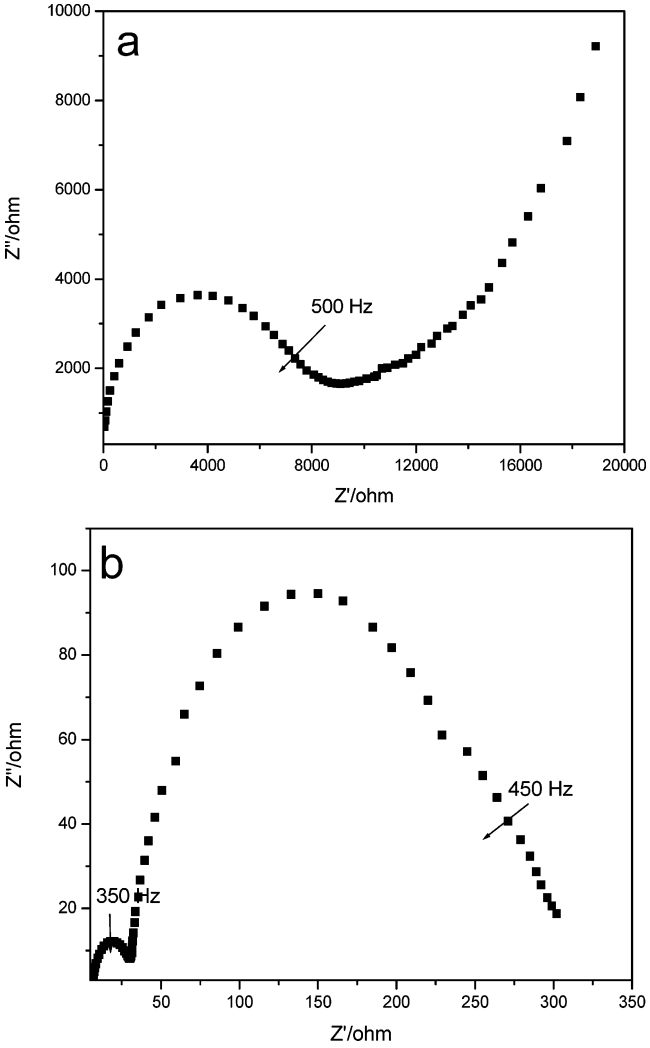

Figure 6. The electrochemical impedance spectra of Bi_2WO_6/ITO electrode during EC (a) and PEC (b) processes. The amplitude of sinusoidal wave was 10 mV, and the frequency range was from 100 kHz to 0.05 Hz.

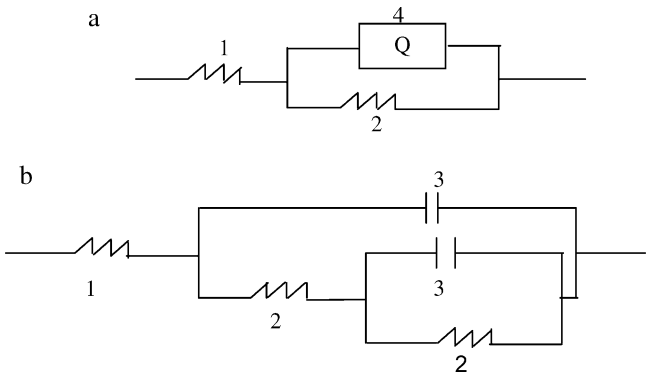

Figure 7. The equivalent circuit diagram of the EIS. (a) Figure 6a; (b) Figure 6b. (1) Diffusion electric resistance; (2) charge-transfer resistance; (3) electric capacity; (4) constant phase element.

reaction. Therefore, the acidity increase of RhB solution can improve the degradation rate of RhB during PEC process. In addition, the shape of the arc did not change in the Nynquist plot with varying pH and concentrations of RhB solution, suggesting that the PEC reaction is a simple electrode process.

Stability of Bi_2WO_6 Nanoplate Film Electrodes. To examine the stability of the Bi_2WO_6 nanoplate film electrode, the PEC process was repeated 5 times with the same electrode.

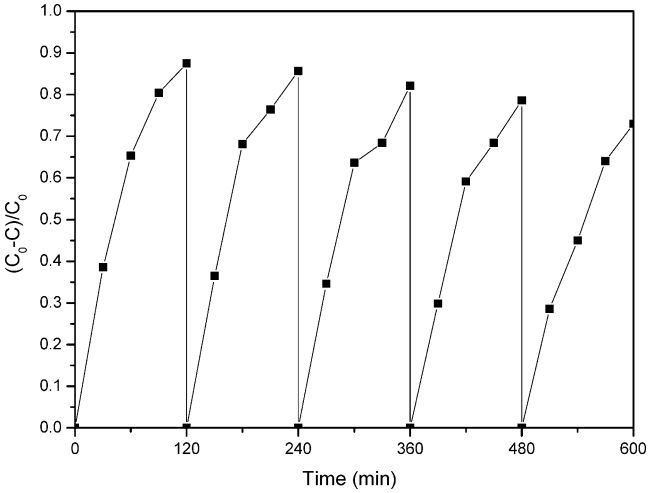

Figure 8. The repeated experiments of photoelectrocatalytic degradation of RhB on the Bi_2WO_6 nanoplate film electrode during PEC process under visible light irradiation (initial concentration of RhB, 5 mg·L^{-1}; irradiation time, 120 min).

Before each experiment, the used Bi_2WO_6 nanoplate film electrode was cleaned with ultrasonication. The results of these repeated experiments showed that Bi_2WO_6 nanoplate film electrode was very stable (Figure 8). There was a slight decrease in degradation efficiency over time as shown in Figure 8. This is because of the contamination of catalyst and peeling of few Bi_2WO_6 nanoplate during PEC process. This decrease can be easily prevented through careful washing of catalyst film and/or compensating the lost Bi_2WO_6 nanoplates.

Degradation Pathway of RhB during PEC Process under Visible Light Irradiation. The degradation process of RhB has been investigated in detail previously. It is well-known that the RhB degradation occurs via two competitive processes: one is N-demethylation, and the other is the destruction of the conjugated structure.[33] The diminishment of the absorption band of RhB solution at 555 nm corresponds to the decomposition of the conjugated xanthene ring in RhB. The absorption band shift of RhB solution toward the blue region suggests the formation of de-ethylated RhB molecule.[34] In our case, no obvious blue-shift of absorbance at 555 nm (corresponding to N-demethylation) was observed during the PEC process (inset of Figure 5). Therefore, we conclude that the degradation of RhB was mainly attributed to the destruction of the conjugated structure. This degradation mechanism of RhB is similar with that in PEC oxidation based on a Ti/TiO_2 mesh electrode.[35]

Conclusions

In this study, we demonstrated that a novel photoelectrochemical (PEC) oxidation system based on a Bi_2WO_6 nanoplate film electrode could efficiently degrade RhB in aqueous solution under visible light ($\lambda > 420$ nm). The Bi_2WO_6 nanoplate film electrode was prepared by a hydrothermal method, combined with a spin coating technique. We observed a significant synergetic effect in degrading RhB via electro-oxidation and photocatalysis under visible light irradiation and proposed a possible mechanism for this synergetic degradation. We believe this study provided an effective approach for aqueous organic pollutants removal by utilizing solar light.

Acknowledgment. This work was supported by National Science Foundation of China (Grants 20503009 and 20673041), and Open Fund of Hubei Key Laboratory of Catalysis and Materials Science (Grants CHCL0508 and CHCL06012).

Supporting Information Available: Nitrogen adsorption−desorption isotherms of the as-prepared Bi_2WO_6 powder, UV−vis absorbance spectra, plots of the $(a)^{1/2}$ versus photon energy ($h\nu$) of the Bi_2WO_6 film on ITO, comparison of hydroxyl radical produced in the PC and PEC processes using tert-butyl alcohol as the chemical reagents, effect of applied bias potentials on the PEC process, and electrochemical impedance spectra of Bi_2WO_6/ITO electrode under different concentrations of RhB solution and different pH during PEC process. The material is available free of charge via the Internet at http://pubs.acs.org.

References and Notes

(1) Kusvuran, E.; Gulnaz, O.; Irmak, S.; Osman, M.; Atanur, H.; Yavuz, I.; Erbatur, O. *J. Hazard. Mater.* **2004**, *109*, 85.
(2) Hoffman, M. R.; Martin, S. T.; Choi, W. *Chem. Rev.* **1995**, *19*, 69.
(3) Candal, R. J.; Zeltner, W. A.; Anderson, M. A. *Environ. Sci. Technol.* **2000**, *34*, 3443.
(4) Vinodgopal, K.; Hotchandani, S.; Kamat, P. V. *J. Phys. Chem.* **1993**, *97*, 9040.
(5) Vinodgopal, K.; Stafford, U.; Gray, K. A.; Prashant, V. K. *J. Phys. Chem.* **1994**, *98*, 6797.
(6) Kesselman, J. M.; Shreve, G. A.; Hoffman, M. R.; Lewis, S. N. *J. Phys. Chem.* **1994**, *98*, 13385.
(7) Hidaka, H.; Shimura, T.; Ajisaka, K.; Sato, S. H.; Zhao, J. C.; Nick, S. *J. Photochem. Photobiol., A: Chem.* **1997**, *109*, 165.
(8) Kim, D. H.; Anderson, M. A. *Environ. Sci. Technol.* **1994**, *28*, 479.
(9) Chih-Cheng, S.; Tse-chuan, C. *J. Mol. Catal. A: Chem.* **2000**, *151*, 133.
(10) Rodríguez, J.; Gómez, M.; Lindquistb, S. E.; Granqvist, C. G. *Thin Solid Films* **2000**, *360*, 250.
(11) Hachem, C.; Bocquillon, F.; Zahraa, O.; Bouchy, M. *Dyes Pigm.* **2001**, *49*, 117.
(12) Davis, R. J.; Gainer, J. L.; Neal, G.; Wu, I. W. *Environ. Res.* **1994**, *66*, 50.
(13) Kiriakidou, F.; Kondarides, D. I.; Verykios, X. E. *Catal. Today* **1999**, *54*, 119.
(14) Panov, G. I.; Uriarte, A. K.; Rodkin, M. A.; Sobolev, V. I. *Catal. Today* **1998**, *41*, 365.
(15) Quan, X.; Yang, S.; Ruan, X.; Zhao, H. *Environ. Sci. Technol.* **2005**, *39*, 3770.
(16) Li, X. Z.; Liu, H. S. *Environ. Sci. Technol.* **2005**, *39*, 4614.
(17) Leng, W. H.; Zhang, Z.; Zhang, J. Q. *J. Mol. Catal. A Chem.* **2003**, *206*, 239.
(18) Hepel, M.; Hazelton, S. *Electrochem. Acta* **2005**, *50*, 5278.
(19) Zhao, X.; Zhu, Y. F. *Environ. Sci. Technol.* **2006**, *40*, 3367.
(20) Solarska, R.; Santato, C.; Jorand-Sartoretti, C.; Ulmann, M.; Augustynski, J. *J. Appl. Eelectrochem.* **2005**, *35*, 715.
(21) Yu, J. G.; Xiong, J. F.; Cheng, B.; Yu, Y.; Wang, J. B. *J. Solid State Chem.* **2005**, *178*, 1968.
(22) Fu, H. B.; Zhang, L. W.; Yao, W. Q.; Zhu, Y. F. *Appl. Catal., B: Environ.* **2006**, *66*, 100.
(23) Fu, H. B.; Pan, C. S.; Zhang, L. W.; Zhu, Y. F. *Mater. Res. Bull.* **2007**, *42*, 696.
(24) Fu, H. B.; Pan, C. S.; Yao, W. Q.; Zhu, Y. F. *J. Phys. Chem. B* **2005**, *109*, 22432.
(25) Zhang, C.; Zhu, Y. F. *Chem. Mater.* **2005**, *17*, 3537.
(26) Tang, J. W.; Zou, Z. G.; Ye, J. H. *Catal. Lett.* **2004**, *92*, 53.
(27) Zhao, X.; Xu, T. G.; Yao, W. Q.; Zhang, C.; Zhu, Y. F. *Appl. Catal., B: Environ.* **2007**, *72*, 92.
(28) Liu, H.; Cheng, S.; Wu, M.; Wu, H.; Zhang, J.; Li, W.; Cao, C. *J. Phys. Chem. A* **2000**, *104*, 7016.
(29) Leng, W. H.; Zhang, Z.; Zhang, J. Q.; Cao, C. N. *J. Phys. Chem. B* **2005**, *109*, 15008.
(30) Lei, P. X.; Chen, C. C.; Yang, J.; Ma, W. H.; Zhao, J. C.; Zang, L. *Environ. Sci. Technol.* **2005**, *39*, 8466.
(31) Chen, C. C.; Zhao, W.; Lei, P. X.; Zhao, J. C.; Serpone, N. *Chem. Eur. J.* **2004**, *10*, 1956.
(32) Wilhelm, P.; Stephan, D. *J. Photochem. Photobiol., A: Chem.* **2007**, *185*, 19.
(33) Chen, C.; Li, X.; Ma, W.; Zhao, J.; Hidaka, H.; Serpone, N. *J. Phys. Chem. B* **2002**, *1062*, 318.
(34) Bao, N.; Feng, X.; Yang, Z.; Shen, L.; Lu, X. *Environ. Sci. Technol.* **2004**, *38*, 2729.
(35) Li, X. Z.; Liu, H. L.; Li, F. B.; Mak, C. L. *J. Environ. Sci. Health* **2002**, *37*, 55.